24th INTERNATIONAL CONGRESS ON SOUND AND VIBRATION
23–27 July 2017, London

THEORETICAL AND EXPERIMENTAL STUDY OF A VIBRATION ISOLATOR USING A NEGATIVE STIFFNESS MAGNETIC SPRING

Yisheng Zheng, Xinong Zhang*, Shilin Xie and Yahong Zhang

State Key Laboratory for Strength and Vibration of Mechanical Structures, Xi'an Jiaotong University, Xi'an 710049, China
email: xnzhang@mail.xjtu.edu.cn

This paper presents a vibration isolator with high-static-low-dynamic stiffness (HSLDS), which is implemented by connecting a negative stiffness magnetic spring (NSMS) in parallel with membranes springs to cancel its positive stiffness. The NSMS consists of two coaxial ring magnets that are axially magnetized and their magnetization directions are the same. In order to achieve the static characteristics of the isolator, the integral expressions of the magnetic force and stiffness produced by the NSMS are firstly gained and they are further approximated by the polynomials. Then the nonlinear dynamic model of the isolator is established and the displacement transmissibility is formulated. Finally, an experimental prototype of the isolator is developed and its isolation performance is tested. The experimental results verify the theoretical results and show that the isolation performance of the isolator with NSMS is superior to that without NSMS.
Keywords: quasi-zero stiffness; magnetic spring; negative stiffness; isolator

1. Introduction

For a linear SODF isolator, the isolation frequency band starts from $\sqrt{2}$ times of its resonance frequency. Hence the stiffness of the isolator needs to be reduced to increase the isolation frequency band, which however would decrease the load bearing capacity. To avoid this contradiction, the so called "high-static-low-dynamic stiffness (HSLDS)" or "quasi-zero stiffness" isolator [1] is proposed. The high-static stiffness can guarantee the load bearing capacity while the low-dynamic stiffness means low resonance frequency. The principle of most HSLDS isolators ever proposed is using negative-stiffness mechanism (NSM) to cancel the positive stiffness of elastic elements. So far all kinds of NSM have been investigated, including inclined springs [1, 2], pre-stressed bar [3, 4], magnetic mechanism [5, 6] and cam-roller-spring [7]. Among these designs, the magnetic mechanism has the advantage of compact configuration, which is important if it is applied in precise instruments.

The authors ever presented a NSMS [6], which consists of two ring magnet magnetized radially. Since the ring magnets magnetized radially is difficult to manufacture, tile magnets magnetized uniformly are employed to assemble the ring magnets. This will inevitably increase the complexity of structures. In this paper, a new kind of NSMS is studied. It also consists of ring magnets, but which are magnetized axially. The ring magnets magnetized axially are easily to be manufacture.

2. Overview of the isolator

The model of the isolator is shown in Fig. 1, where Fig. 1(a) shows the 3D model of the isolator and Fig. 1(b) illustrates the section view of the isolator. The isolator mainly consists of two membrane springs and a negative stiffness magnetic spring (NSMS). The membrane springs are used to provide positive stiffness for the isolator and can undertake the static load. Another function of the membrane springs is that they can constrain the isolated mass to move in the axial direction. The stiffness of the membrane spring can be seen to be constant when the displacement of the isolated mass is small enough. The NSMS is composed of two ring magnets, which are magnetized in the axial direction. After appropriate design, the center of the inner magnet should coincide with that of the outer magnet when the isolator is at the static equilibrium state. At this position, the NSMS can produce large negative stiffness to cancel the positive stiffness of the membrane springs while generating zero magnetic force so as not to affect the load bearing capacity of the membrane springs. This means that the isolator can have the characteristic of "high-static-low-dynamic stiffness (HSLDS)".

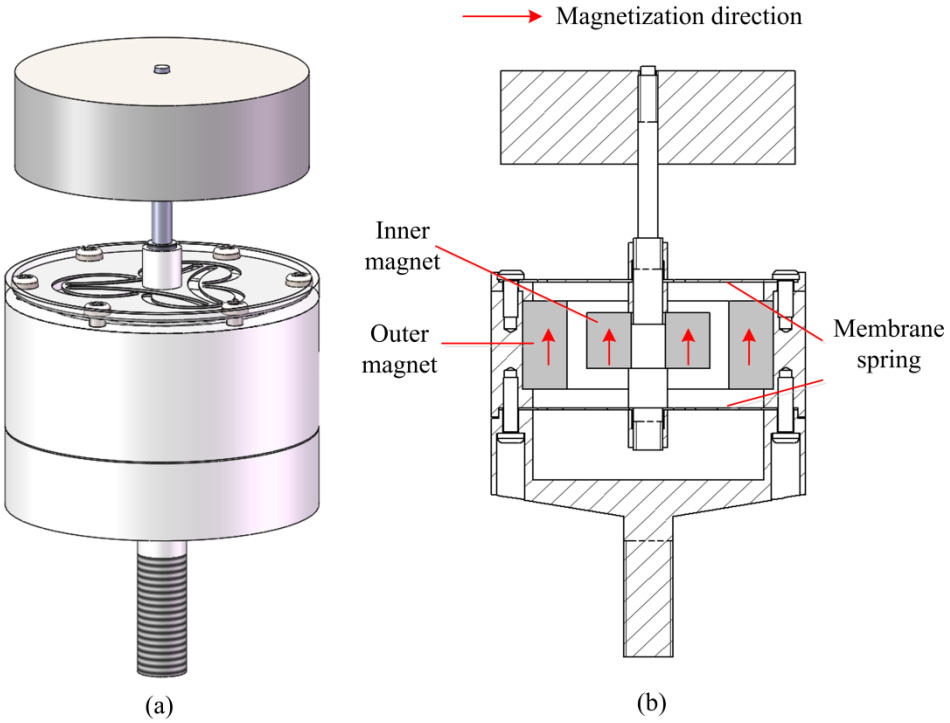

Fig.1 Schematic model of the isolator: (a) 3D model; (b) section view of the isolator

3. Magnetic force and stiffness of the negative stiffness magnetic spring (NSMS)

The implementation of the characteristic of high-static-low-dynamic stiffness mainly depends on the NSMS. Hence it is necessary to acquire its magnetic force and stiffness. The Amperian current model and the Coulombian model are usually employed to derive the magnetic field [8]. The former model says that the magnets can be expressed by the equivalent current in the volume and on the surface while the latter claims that the magnets can be replaced by the equivalent charge in the volume and on the surface. Here the formulation in reference [9] will be adopted, which is obtained based on the Coulombian model.

The residual magnetic flux density of the magnets is B_r. The geometric parameters of the magnets are expressed in Fig. 2. The formulation of the magnetic force and stiffness are given as

$$
\begin{aligned}
F_m = &+\int_{\theta_1=0}^{2\pi}\int_{\theta_2=0}^{2\pi}\int_{r_1=r_{i1}}^{r_{o1}}\int_{r_2=r_{i2}}^{r_{o2}} (l_1-l_2+y)\cdot a(l_1-l_2+y)\cdot r_1 r_2 \mathrm{d}r_1\mathrm{d}r_2\mathrm{d}\theta_1\mathrm{d}\theta_2 \\
&+\int_{\theta_1=0}^{2\pi}\int_{\theta_2=0}^{2\pi}\int_{r_1=r_{i1}}^{r_{o1}}\int_{r_2=r_{i2}}^{r_{o2}} (l_2-l_1+y)\cdot a(l_2-l_1+y)\cdot r_1 r_2 \mathrm{d}r_1\mathrm{d}r_2\mathrm{d}\theta_1\mathrm{d}\theta_2 \\
&-\int_{\theta_1=0}^{2\pi}\int_{\theta_2=0}^{2\pi}\int_{r_1=r_{i1}}^{r_{o1}}\int_{r_2=r_{i2}}^{r_{o2}} (l_2+l_1+y)\cdot a(l_2+l_1+y)\cdot r_1 r_2 \mathrm{d}r_1\mathrm{d}r_2\mathrm{d}\theta_1\mathrm{d}\theta_2 \\
&-\int_{\theta_1=0}^{2\pi}\int_{\theta_2=0}^{2\pi}\int_{r_1=r_{i1}}^{r_{o1}}\int_{r_2=r_{i2}}^{r_{o2}} (-l_2-l_1+y)\cdot a(-l_2-l_1+y)\cdot r_1 r_2 \mathrm{d}r_1\mathrm{d}r_2\mathrm{d}\theta_1\mathrm{d}\theta_2
\end{aligned} \tag{1}
$$

$$
\begin{aligned}
K_m &= -\frac{\partial F_z}{\partial y} \\
&= -\int_{\theta_1=0}^{2\pi}\int_{\theta_2=0}^{2\pi}\int_{r_1=r_{i1}}^{r_{o1}}\int_{r_2=r_{i2}}^{r_{o2}} (a(l_1-l_2+y)-3(l_1-l_2+y)^2\cdot f(l_1-l_2+y))\cdot r_1 r_2 \mathrm{d}r_1\mathrm{d}r_2\mathrm{d}\theta_1\mathrm{d}\theta_2 \\
&-\int_{\theta_1=0}^{2\pi}\int_{\theta_2=0}^{2\pi}\int_{r_1=r_{i1}}^{r_{o1}}\int_{r_2=r_{i2}}^{r_{o2}} (a(l_2-l_1+y)-3(l_2-l_1+y)^2\cdot f(l_2-l_1+y))\cdot r_1 r_2 \mathrm{d}r_1\mathrm{d}r_2\mathrm{d}\theta_1\mathrm{d}\theta_2 \\
&+\int_{\theta_1=0}^{2\pi}\int_{\theta_2=0}^{2\pi}\int_{r_1=r_{i1}}^{r_{o1}}\int_{r_2=r_{i2}}^{r_{o2}} (a(l_2+l_1+y)-3(l_2+l_1+y)^2\cdot f(l_2+l_1+y))\cdot r_1 r_2 \mathrm{d}r_1\mathrm{d}r_2\mathrm{d}\theta_1\mathrm{d}\theta_2 \\
&+\int_{\theta_1=0}^{2\pi}\int_{\theta_2=0}^{2\pi}\int_{r_1=r_{i1}}^{r_{o1}}\int_{r_2=r_{i2}}^{r_{o2}} (a(-l_2-l_1+y)-3(-l_2-l_1+y)^2\cdot f(-l_2-l_1+y))\cdot r_1 r_2 \mathrm{d}r_1\mathrm{d}r_2\mathrm{d}\theta_1\mathrm{d}\theta_2
\end{aligned} \tag{2}
$$

respectively, where

$$
\begin{aligned}
a(\xi) &= \frac{\sigma_1\sigma_2}{4\pi\mu_0}\frac{1}{(r_1^2+r_2^2-2r_1r_2\cos(\theta)+\xi^2)^{3/2}} \\
f(\zeta) &= \frac{\sigma_1\sigma_2}{4\pi\mu_0}\frac{1}{(r_1^2+r_2^2-2r_1r_2\cos(\theta)+\xi^2)^{5/2}}
\end{aligned} \tag{3}
$$

σ_1 and σ_2 are the surface magnetic pole density, $\sigma_1=\sigma_2=B_r$; μ_0 is the vacuum permeability; y is the displacement of the inner magnet relative to the outer magnet. The formulations shown as Eqs. (1), (2) can be solved by numerical integration.

The geometric parameters of the NSMS have great influence on its force and stiffness characteristic. Hence it is necessary to optimize the geometric parameters considering the following factors: the value of negative stiffness; the effective stroke length; the nonlinearity of the magnetic stiffness. The negative stiffness should match the positive stiffness; the effective stroke length should be large; the nonlinearity of stiffness should be as weak as possible. Fig. 3 shows the achieved magnetic force and stiffness of the NSMS. In the range of -3 ~3 mm, the magnetic stiffness is nearly constant. This can be seen as the effective stroke length of the NSMS, where it can cancel the positive stiffness of the membrane springs without bringing obvious nonlinear effect. Fig. 3(a) shows that the magnetic force curve can be fitted by a cubic polynomial curve approximately, presented as

$$
F_m = k_1 y + k_3 y^3 \tag{4}
$$

where k_1=5700 N/m and $k_3 = -1.6\times10^7$ N/m^3.

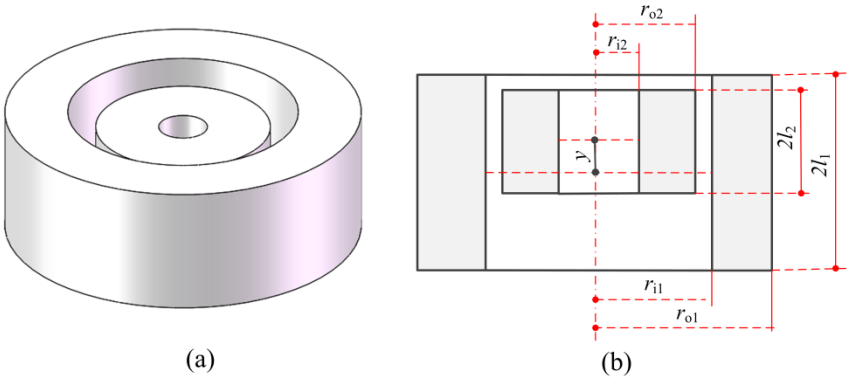

Fig. 2 Geometric parameters of the magnetic spring: (a) 3D model of the magnetic spring; (b) section view of the magnetic spring

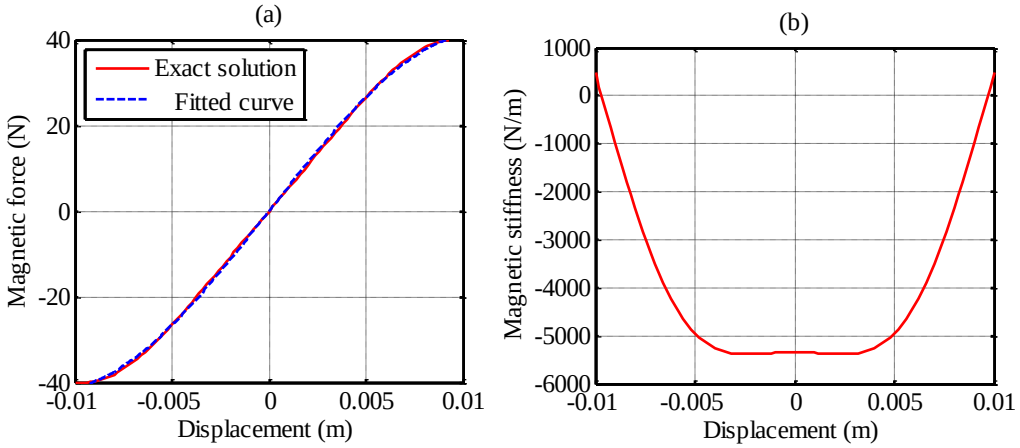

Fig. 3 Magnetic force (a) and magnetic stiffness (b) of the magnetic spring with parameters: r_{o1}=25.5 mm, r_{i1}=16.5 mm, r_{o2}==10 mm, r_{i2}=3.5 mm, $2l_1$=19 mm, $2l_2$=6 mm, B_r=1.35 T

4. Dynamic analysis

The restoring force of the isolator due to the membrane springs and the magnetic spring is

$$F_r = (k_e - k_1)y - k_3 y^3 \tag{5}$$

where k_e is the stiffness of the membrane springs. For the SODF nonlinear isolator, when under base displacement excitation $x_0 = X_0 \cos(\omega t + \theta)$, the dynamic equation is

$$m\ddot{y} + c\dot{y} + (k_e - k_1)y - k_3 y^3 = -m\ddot{x}_0 \tag{6}$$

y is the displacement of the isolated mass relative to the base and its absolute displacement is

$$x = x_0 + y \tag{7}$$

The dimensionless form of Eq. (6) is

$$u'' + 2\xi u' + u + \delta u^3 = \beta^2 \cos(\beta\tau + \theta) \tag{8}$$

where

$$\begin{aligned} &u = y / X_0, \tau = \omega_n t, \omega_n = \sqrt{(k_e - k_1)/m}, \\ &\xi = c/(2m\omega_n), \delta = -k_3 {X_0}^2/(k_e - k_1), \beta = \omega/\omega_n \end{aligned} \tag{9}$$

The Duffing equation Eq. (8) can be solved using the Harmonic Balance method. The detailed procedure to solve this equation can be referred in [6]. Here only the formulation of the transmissibility is given

$$T = \sqrt{1 + U^2 + \frac{2U}{\beta^2}(\beta^2 U + U + \frac{3}{4}\delta U^3)} \tag{10}$$

where

$$\beta^2 = \frac{U^2(4 + 3\delta U^2) - 8(\xi U)^2 \pm \sqrt{(8\xi^2 U^2 - 4U^2 - 3\delta U^4)^2 - (U^2 - 1)(4U + 3\delta U^3)^2}}{4(U^2 - 1)} \tag{11}$$

and U is the amplitude of u, namely $u = U\cos(\beta\tau)$. If the base excitation is small enough, the nonlinearity of the dynamic equation is weak and the transmissibility can be simplified as

$$T = \sqrt{\frac{(k_e - k_1)^2 + (c\omega)^2}{(k_e - k_1 - m\omega^2)^2 + (c\omega)^2}} \tag{12}$$

5. Experiment investigation

An experimental prototype is built to validate the better isolation performance of the proposed isolator. Figure. 4 shows the photograph of the experiment. The magnet material is NdFeB, which has strong magnetism. The material of the other structure is aluminum or steel with low permeability. The parameters of the magnetic spring and its static characteristic are as shown in Fig. 3. The isolated mass is 0.466 Kg.

When testing the transmissibility, the isolator is installed on a shaking table, which is excited by an electromagnetic exciter. The PULSE analyzer can generate an exciting signal for the electromagnetic exciter, which is amplified by the Power amplifier. Two accelerometers are placed on the isolated mass and the shaking table respectively. The obtained accelerations are then input to the PULSE analyzer for analysis.

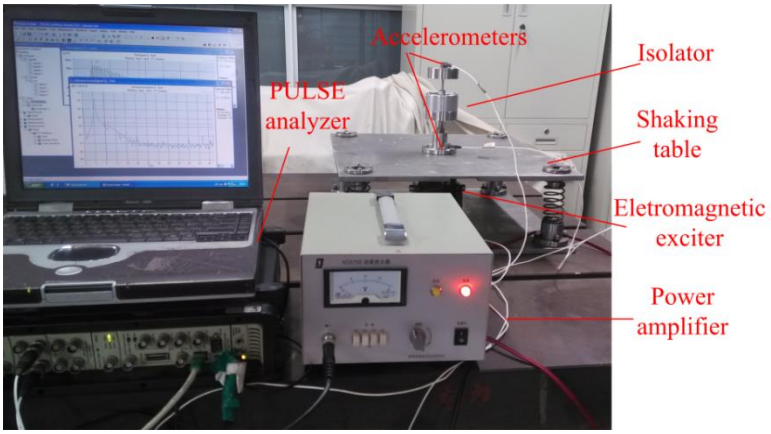

Fig. 4 Photograph of the experiment to test the transmissibility of the isolator

A rand excitation is input to the electromagnetic exciter. In order to ensure that the nonlinear effect of the isolator is not induced, the excitation is set to be small. Two cases are conducted: the isolator with the NSMS and that without the NSMS. The experimental results are shown in Fig. 5. The experimental resonance frequency of the isolator without NSMS is 18.6 Hz while that with NSMS is 5.3 Hz. Accordingly, the isolation frequency band is increased from (>26.1 Hz) to (>7.6 Hz). Also the peak transmissibility is decreased by 11 dB. Hence the isolation performance of the proposed isolator with NSMS is really superior to that without NSMS.

In Fig. 5, the analytical transmissibility of the isolator with NSMS is obtained using Eq. (12) and it has good coincidence with the experimental results. In the analytical calculation, the stiffness of the membrane springs and the damping are identified based on the experimental transmissibility in the case without NSMS.

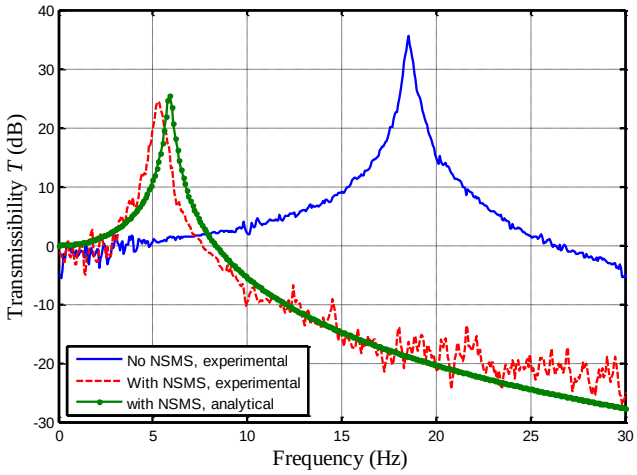

Fig. 5 Transmissibility of the isolator

6. Conclusions

In this paper, a negative stiffness magnetic spring (NSMS) is proposed, which is utilized to reduce the stiffness of the isolator and hence improve its isolation performance. The NSMS is superior to other negative stiffness mechanisms like inclined springs and pre-stressed bars due to its compact configuration. The proposed isolator is then investigated analytically and experimentally. The experimental results show that the resonance frequency is reduced to 5.3 Hz from 18.6 Hz and the peak transmissibility is also decreased by 11 dB, which demonstrates that the isolator with NSMS has great advantage over that without NSMS.

REFERENCES

1 Carrella, A., Brennan, M. J. and Waters, T. P. Static analysis of a passive vibration isolator with quasi-zero-stiffness characteristic, *Journal of Sound and Vibration*, **301** (3–5), 678-689, (2007).

2 Le, T. D. and Ahn, K. K. A vibration isolation system in low frequency excitation region using negative stiffness structure for vehicle seat, *Journal of Sound and Vibration*, **330** (26), 6311-6335, (2011).

3 Platus, D. L. Negative-stiffness-mechanism vibration isolation systems, *Proceedings of SPIE1619, Vibration Control in Microelectronics Optics, and Metrology*, 44–54, (1991).

4 Huang, X., Liu, X., Sun, J., Zhang, Z. and Hua, H. Vibration isolation characteristics of a nonlinear isolator using Euler buckled beam as negative stiffness corrector: A theoretical and experimental study, *Journal of Sound and Vibration*, **333** (4), 1132-1148, (2014).

5 Wu, W., Chen, X. and Shan, Y. Analysis and experiment of a vibration isolator using a novel magnetic spring with negative stiffness, *Journal of Sound and Vibration*, **333** (13), 2958-2970, (2014).

6 Zheng, Y., Zhang, X., Luo, Y., Yan, B. and Ma, C. Design and experiment of a high-static–low-dynamic stiffness isolator using a negative stiffness magnetic spring, *Journal of Sound and Vibration*, **360**, 31-52, (2016).

7 Zhou, J., Wang, X., Xu, D. and Bishop, S. Nonlinear dynamic characteristics of a quasi-zero stiffness vibration isolator with cam–roller–spring mechanisms, *Journal of Sound and Vibration*, **346**, 53-69, (2015).
8 Ravaud, R. and Lemarquand, G. Comparison of the coulombian and amperian current models for calculating the magnetic field produced by radially magnetized arc-shaped permanent magnets, *PIER-Progress In Electromagnetics Research*, **95**, 309, (2009).
9 Ravaud, R., Lemarquand, G. and Lemarquand, V. Force and Stiffness of Passive Magnetic Bearings Using Permanent Magnets. Part 1: Axial Magnetization, *Magnetics, IEEE Transactions on*, **45** (7), 2996-3002, (2009).